Available online at www.sciencedirect.com

ScienceDirect

Procedia Structural Integrity 75 (2025) 311–317

Structural Integrity Procedia

www.elsevier.com/locate/procedia

Fatigue Design 2025 (FatDes 2025)

Material mechanisms of the nanostructured metallic multilayer post-weld treatment for fatigue strength increase

Niclas Spalek[a]*, Mohsen Falah[a], Maren Seidelmann[a], Nikolay Lalkovski[a], Guilherme Abreu Faria[b], Marcus Rutner[a]

[a]*Hamburg Institute of Technology, Denickestraße 17, 21073 Hamburg, Germany*
[b]*Helmholtz-Zentrum hereon GmbH, Max-Planck-Straße 1, 21502 Geesthacht, Germany*

Abstract

While traditional post weld treatments intend to reduce the fatigue failure potential by changing the weld seam geometry, introduction of compressive residual stresses and shielding off environmental impacts, the novel nanostructured metallic multilayer (NMM) post-weld treatment covers all three mechanisms simultaneously. NMM offer combined high strength and ductility and a significantly enhanced fatigue resistance. In a recent study a strong enhancement in fatigue resistance was detected. Utilizing energy-dispersive X-Ray diffraction techniques at the P61A-beamline at the German Synchrotron (DESY), it was found that residual stresses generated during the deposition process play a crucial role in this enhancement. Specifically, tensile stresses within the nanolaminate induce beneficial compressive stresses in the underlying substrate, effectively inhibiting fatigue crack initiation and resulting in an unprecedented increase in fatigue strength. NMM treatment of the double-V weld increases the fatigue strength from FAT class 80 to 225. This paper investigates which process parameters optimize the compressive stress profile in the steel base material, paving the way for the NMM post-weld treatment to reliably and economically contribute to longevity of cyclically loaded metal infrastructure.

Peer-review under the responsibility of Dr Fabien Lefebvre with at least 2 reviewers per paper

Keywords: fatigue, lifetime extension, electrodeposition, NMM, XRD, thin film, multilayer

Peer-review under the responsibility of Dr Fabien Lefebvre with at least 2 reviewers per paper
10.1016/j.prostr.2025.11.032

1. Introduction

In light of the climate changing for the worse and resource shortage, efforts to increase the usable lifetime of engineering structures become more important. Fatigue is highly responsible for premature failure of joints, components and structures and has significant implications for the design and longevity of infrastructure subjected to cyclic loading. Welded joints, which are found in more than half of all civil engineering products (Aucott et al., 2017), are in most cases critical positions where fatigue cracks initiate, posing risks to the structural integrity and functionality of the steel structure. As a result, improving the fatigue resistance of these welded connections is vital for ensuring the longevity and safety of metal infrastructure. The development of advanced post-weld treatment methods presents a crucial step towards more sustainable and resource-efficient structures. However, traditional post-weld treatments (Kuhlmann et al., 2005; Ummenhofer et al., 2009, 2005) achieved only limited improvement in fatigue strength, thus preventing widespread use of these conventional methods.

A novel post-weld treatment (PWT) has been introduced in the form of a nanostructured metallic multilayer (NMM) applied on the welded (double-V-weld) butt joint (Brunow et al., 2022; Brunow and Rutner, 2021). The effects and implications for the welded monopile foundation of offshore wind energy plants have been explored (Brunow et al., 2023). This paper seeks to investigate the effects of process parameters on the NMM and its interaction with the steel substrate, specifically to establish a measure to tailor residual stresses (RS) in the steel substrate adjacent to the surface in order to maximize the fatigue strength increase, hence the lifetime of infrastructure.

NMM is a surface treatment of the welded joint is applied onto the surface. Hence, the NMM develops its effect at the surface and adjacent to the surface which are the critical areas in respect to fatigue. Cracks mostly initiate at the surface and propagate into the material. The NMM has a micrometer thickness and does not lead to stiffness change, compared to other strengthening methods, such as Fiber Metal Laminates (Woelke et al., 2015). The NMM thin film does not contribute in carrying any internal forces, but induces compressive stresses at and adjacent to the steel surface suppressing dents and microcracks. The NMM post-weld-treatment has been developed over the last years from small-scale laboratory tests (Brunow and Rutner, 2021; Brunow et al., 2021; Ramezani et al., 2017) to a scalable technology (Brunow et al., 2022) by using electrodeposition, applicable for new and existing structures (Rutner et al., 2024; Rutner et al., 2025; Seidelmann et al., 2025) as well as for metal 3D-printed structures (Falah et al., 2025).

Welding and subsequent cooling causes residual stresses due to warpage, shrinkage, phase transition, grain growth and geometric inhomogeneities (Chmelko et al., 2018; Hensel et al., 2015; Totten, 2008). Conventional post-weld treatments try to change the geometry of the weld by grinding or remelting (Al-Karawi and Al-Emrani, 2021). Alternatively, PWT introduce compressive stresses into the steel adjacent to the surface reducing localized stress concentrations during cyclic loading and thereby enhancing the fatigue performance (Kuhlmann et al., 2005; Ummenhofer et al., 2009). As a third measure, protective coatings shield the weld off environmental conditions.
Electrodepositing a Cu/Ni NMM onto the weld and the HAZ greatly increases the fatigue strength of the connections, as demonstrated before (Brunow et al., 2023). The underlying mechanism is believed to be highly depending on the residual stress states at and adjacent to the surface. During electrodeposition, residual stresses are formed as a result of grain growth and coalescence, which can be controlled by tailoring the influential parameters (Chason et al., 2013, 2002; Engwall et al., 2016).

This paper evaluates which process conditions are beneficial for residual stress build-up and enhancing the fatigue strength of double-V (DV) welded dog-bone samples.

2. Materials and Methods

S355 J2 mild steel plates are welded together by using a DV butt-weld. MAG-welding is performed by a Lorch 5 XT controlled by a UR10e robot. The Böhler Q G3Si1/SG2 is used as filler material. The dog-bone samples are cut from the welded steel plates by waterjet-cutting. The dimensions are 280x25x8 mm^3 and in accordance with (*DIN 50125:2022-08*, 2022) sample type E. Tensile-tensile fatigue testing is performed and evaluated according to (*DIN 50100:2016-12*, 2016) on a servo-hydraulic uni-axial testing machine (Schenck PC400M) with a frequency of 8 Hz and stress ratio R=0. Before deposition of the NMM, a special sample pre-treatment removes any oxides, scales, contamination or grease. In the following, two sample sets are distinguished, the sample set *DC NMM* and the sample set *PC NMM*. For sample set *DC NMM*, surface pre-treatment is performed via abrasively grinding the samples with

grit 80 to a metal shine finish followed by ultrasonic cleaning before electrodeposition of the NMM. In contrast, sample set *PC NMM* is clean blasted using steel spheres (S110 by MHG) with 6,5 bar to remove any residue followed by ultrasonic cleaning and electrodeposition of the NMM.

Electrodeposition is controlled by a galvanostat pulse plating power supply (Plating Electronics pe86CB-20-5-25-SGD). The Ni/Cu sulphate-based electrolyte according to Bonhôte and Landolt (1997) is used in a single-bath configuration to achieve a multilayered cross section by controlling the current densities and deposition times of the respective nanolayers. A total thickness of 9000 nm is deposited, consisting of a 1000 nm Ni-base layer for optimal adhesion between the steel-based substrate and the multilayered Copper and Nickel films. While for *DC NMM* a direct current is applied for each layer, for *PC NMM* the current is supplied in high-frequency pulses. Detailed information about the electrodeposition parameters is summarized in Table 1.

Table 1. Sample preparation and NMM process parameters.

Sample set	*As-welded*	*DC NMM*	*PC NMM*
Sample pre-treatment	-	80 grit grinding	S110 clean blasting
Total NMM thickness [nm]	-	9000	9000
Nickel levelling layer thickness [nm]	-	1000	1000
Copper layer thickness [nm]	-	15	5
Nickel layer thickness [nm]	-	35	35
Average Copper current density [mA cm^{-2}]	-	0,45	0,2
Average Nickel current density [mA cm^{-2}]	-	22	7
Pulse frequency [Hz]	-	-	20
Duty cycle [%]	-	-	10

Energy Dispersive X-Ray Diffraction (EDXRD) is performed at the P61A white beam beamline of PETRA-III at DESY in Hamburg. To ensure full sample penetration and rapid data acquisition, a broad energy spectrum ranging from 30 to 200 keV is utilized. The experimental setup included two independently positioned point detectors at angles of $2\theta_0 = 5{,}8°$ horizontally and $2\theta_1 = 4{,}5°$, vertically. Measurements are taken at 10 µm intervals across the specimen cross section, with collimator slits adjusted accordingly. A total of 25 data points along the depth are collected for each sample, covering up to 250 µm in depth measured from the surface. The experiments are conducted in transmission mode. For the energy dispersive experiment, standard Bragg's law can be rearranged to

$$d(hkl) = \frac{hc}{2\sin\theta_d}\frac{1}{E(hkl)} = const\,\frac{1}{E(hkl)} \tag{1}$$

During subsequent stress analysis, shear stresses are set to 0 as well as out-of-plane strains, therefore the fundamental equation of X-Ray stress analysis becomes

$$\varepsilon_{11}(hkl) = \frac{1}{2}s_2\sigma_{11} + s_1(\sigma_{11} + \sigma_{33}) \tag{2}$$

$$\varepsilon_{33}(hkl) = \frac{1}{2}s_2\sigma_{33} + s_1(\sigma_{11} + \sigma_{33}) \tag{3}$$

3. Results

3.1 Fatigue performance

Tension-tension fatigue testing (constant amplitude loading) is performed with *as-welded* samples and with samples after *NMM* deposition, both for *direct current (DC)* and *pulsed current (PC)* plating. The stress ratio is R = 0. The S-N curves for the mean (dashed lines) $\Delta\sigma_{R,50\%}$ and the 5% quantile (solid lines) $\Delta\sigma_{R,5\%}$ are shown in Figure 1. Run-outs are considered samples exceeding 2,5 × 10^6 cycles to failure. The slope of the S-N curve of the *as-welded* sample set is set to k = 3 in accordance with (*DIN EN 1993-1-9*, 2010). The resulting fatigue strength is 79 MPa, hence, consistent with the FAT class of the DV butt-welded joint of 80. In the welding notch class catalogue of *DIN EN 1993-1-9*, the highest FAT class 160 corresponds to the base material. The fatigue tests of the *DC NMM* data set

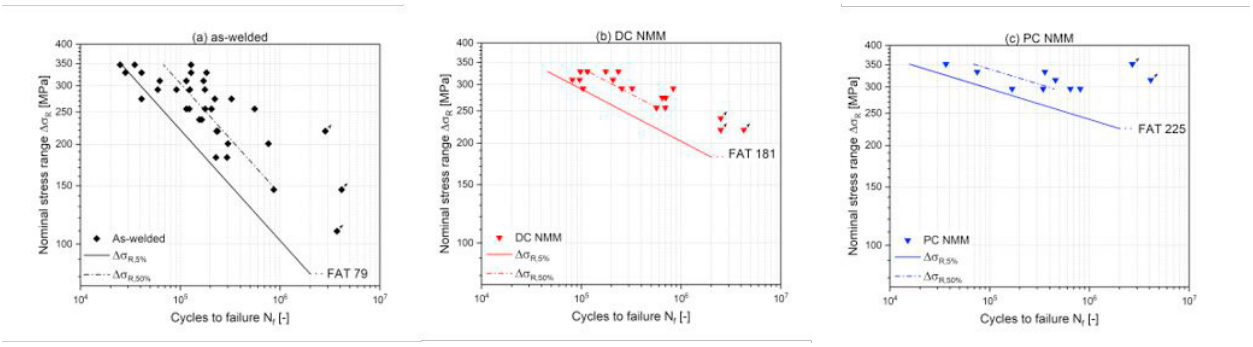

Figure 1. S-N curves and their mean (dashed line) and 5%-quantile (solid line) for sample sets (a) As-welded, (b) DC NMM and (c) PC NMM. Annotation of their respective FAT classes.

yields to an increased FAT class of 181, far exceeding conventional post-weld treatments (Haagensen and Maddox, 2013; Marquis and Barsoum, 2016), as shown in Fig. 1(b). The notable decrease in inherent variance, as illustrated by the reduced scatter of data points, has contributed to the elevation of the FAT class. The reduced scatter, hence the smaller distance between the mean $\Delta\sigma_{R,50\%}$ and 5%-quantile $\Delta\sigma_{R,5\%}$, is interpreted as a high level of reproducibility and reliability of the NMM technology. The slope of the S-N curve is reduced to m = 6.3, confirming lower fatigue-criticality of the NMM post-weld treated weld compared to the *as-welded* condition. More data are needed to verify the exact endurance limit, however only run-outs are detected at nominal stress levels below 0.7 f_y, as shown in Fig. 1(b).

For the sample set *PC NMM* the fatigue data show an even further increased FAT class 225, exceeding the results of the *DC NMM* sample set. The slope is reduced to m = 10.8. More data are needed to confirm the endurance limit.

Surprisingly, run-outs are observed for stress levels up to 90% of the yield strength f_y of the substrate steel. Table 2 presents the factorial increases of lifetime in dependence of the applied maximum stress range. For the stress range of 0.8 f_y a fourfold increase in lifetime for the butt-welded samples is achieved. In case the applied maximum stress levels are smaller, the lifetime increases even more, indicated by the low S-N gradient in Figure 1(c).

Table 2. Lifetime increase of $\Delta\sigma_{R,50\%}$ of both NMM sample sets.

Stress range	As-welded	DC NMM	PC NMM
0.9 f_y ≙ 330 MPa	1	1.44	1.71
0.8 f_y ≙ 296 MPa	1	2.17	4.00

3.2 X-Ray stress analysis

In Brunow et al. (2023) hypotheses for the underlying mechanisms for increased lifetime are presented, with a particular focus on residual stresses. This paper explores the influence of the RS in detail. Previous research by Clemens et al. (1999) and Nix and Clemens (1999) has demonstrated that tensile residual stresses develop within the thin film during the electrodeposition process. Consequently, through stress equilibration, residual compressive stresses form in the steel surface. This redistribution of residual stresses mitigates notch criticality in the weld toes. In order to verify the hypothesis, EDXRD measurements are conducted, to measure and quantify the residual stress distribution across the depth and adjacent to the surface. **Erreur ! Source du renvoi introuvable.** presents the residual stresses across the thickness in the steel substrate. The residual stress distribution in the s_{11}-direction of the *as-welded* condition is not uniform but varies. While at the steel surface and adjacent to the surface residual compressive stress is measured, the cross section also reveals residual tensile stress up to a maximum of $\sigma_{11,\text{ as-welded, max}}$ = 326 MPa. These reference stresses are in line with observations in the literature (Hensel et al., 2015; Trojan et al., 2017) which describe complex stresses forming after welding as a result of warpage, impeded shrinkage, phase transformations and grain growth.

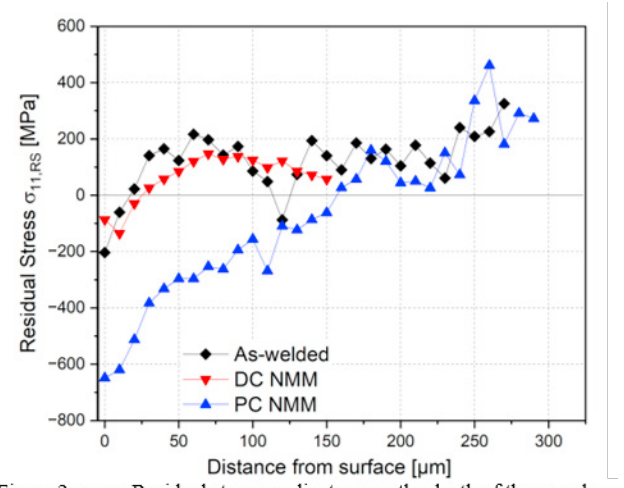

Figure 2. $\sigma_{11,RS}$ Residual stress gradient across the depth of the sample.

DC NMM changes the residual stress distribution only marginally. The residual compressive stress extends further into the substrate.

In contrast, *PC NMM* treatment leads to a significant enhancement in the compressive stress profile. This enlarged profile extends to a depth of $d_{PC,0}$ = 157 µm into the steel substrate. The highest residual compressive stress is measured at the surface of the steel substrate and amounts to $\sigma_{11,\text{ PC NMM, min}}$ = -650 MPa. The σ_{11} direction points along the tensile load direction.

4. Discussion

The results from fatigue testing demonstrate a significant enhancement in the notch class, progressing from FAT 79 for the *as-welded* samples to FAT 181 for *DC NMM* and to FAT 225 for *PC NMM*-treated samples. This increase in fatigue strength surpasses the notch class of the base material, FAT class 160 according to DIN EN 1993-1-9:2010-12. Notably, for *PC NMM*, the residual compressive stress profile substantially increases compared to the *as-welded* samples or the *DC NMM* treated samples. An increase of the residual compressive stress profile is seen as a cause to postpone or even prevent the crack initiation at the surface. Hence, the RS compressive stress profile correlates with the fatigue strength increase and the extended lifetime.

However, comparing the data between the *as-welded* and *DC NMM* samples, RS development does not seem to fully explain the substantial increase in fatigue strength from FAT class 79 to 181, even though a marginal change in RS is detectable. Lifetime increases have been discussed and reported in the literature by exploring the effects of a hard coating (Stoudt et al., 2001; Wang et al., 2006; Zhu and Zhang, 2009). Further investigation is necessary to assess the influence of RS profile changes and potential additional mechanisms and the correlation with fatigue strength.

For *PC NMM,* the residual compressive stress profile extends up to a depth of $d_{PC,0}$ = 157 µm. It is noted that superposing effects of the NMM-treatment and the clean blasting can be expected. Clean blasting and shot peening are regarded as PWT (Hensel et al., 2019; Kim and Jeong, 2013; Scholtes and Vöhringer, 1993; Soyama et al., 2021) which introduce residual compressive stresses into the treated material enhancing the fatigue strength. Moreover, pulsed current plating further contributes to an increase in residual stresses within the thin film, surpassing those induced by DC plating (Abadias et al., 2018; Engwall et al., 2016; Shugurov and Panin, 2020). These findings are

used herein to interpret the residual stresses in multilayer and substrate. It can be deducted that the *PC NMM* provides higher residual compressive stresses than the *DC NMM*.

Surprisingly, the absolute values for the residual compressive stresses $\sigma_{11,\,PC\,NMM,\,min}$ = -650 MPa even exceed the yield strength of the base material f_y = 355 MPa, which is attributed on the one hand to strain hardening during sample preparation by means of clean blasting, on the other hand by a three-dimensional compressive stress state in the steel substrate created under the effect of the thin multilayer and the surrounding material inhibiting dislocation movement.

5. Conclusions

The nanostructured metal multilayer (NMM) treatment of the double-sided V butt-welded joint results in significant increase of fatigue strength. This study explores residual compressive stresses which are seen as one leading underlying mechanism for the fatigue strength increase. Further, process parameters for the NMM deposition are varied. Two sample sets, one with the NMM deposited with direct current, and the other one with NMM deposited with pulsed current, are compared among each other and with the as-welded (reference) sample set in respect to residual stress distribution along the depth and fatigue strength.

The fatigue results of the *as-welded* condition align with the notch class of 80 for a double-sided butt-welded joint as defined in the literature. Deposition of a Cu/Ni nanolaminate on the weld by using direct current (*DC NMM*) drastically increases the fatigue strength to a FAT class 181, well above the fatigue strength of the base material, FAT class 160 as defined by DIN EN 1993-1-9:2010-12. Subsequent improvements in the processing of the NMM on the weld, namely the application of pulsed current plating and prior clean blasting pre-treatment, further increases the notch class to FAT class 225. Run-outs are seen at a stress range of 80-90% of the yield strength which could be a first indicator of a high endurance limit. Measurements of the residual compressive stress profiles along the depth of the specimen reveal that the residual stress state post-welding is transferred to a residual compressive stress profile during NMM deposition. While direct current NMM deposition may only marginally changes the residual compressive stress profile, it is dramatically increased by using pulsed current NMM deposition. A clear correlation of the size and shape of the residual compressive stress profile and the achievable fatigue strength is seen. Further investigation is needed to quantify the effect of the residual stresses induced by NMM in comparison to other mechanisms, such as hardness of the coating.

Acknowledgements

The authors acknowledge DESY, Hamburg - a member of the Helmholtz Association HGF - for positively evaluating the proposal I-20230348, with special thanks to Dr. Abreu-Faria for his assistance as the beamline scientist.

References

Abadias, G., Chason, E., Keckes, J., Sebastiani, M., Thompson, G.B., Barthel, E., Doll, G.L., Murray, C.E., Stoessel, C.H., Martinu, L., 2018. Review Article: Stress in thin films and coatings: Current status, challenges, and prospects. J. Vac. Sci. Technol. A 36. https://doi.org/10.1116/1.5011790.

Al-Karawi, H., Al-Emrani, M., 2021. The efficiency of HFMI treatment and TIG remelting for extending the fatigue life of existing welded structures. Steel Constr. 14, 95–106. https://doi.org/10.1002/stco.202000053.

Aucott, L., Huang, D., Dong, H.B., Wen, S.W., Marsden, J.A., Rack, A., Cocks, A.C.F., 2017. Initiation and growth kinetics of solidification cracking during welding of steel. Sci. Rep. 7, 40255. https://doi.org/10.1038/srep40255.

Bonhôte, Ch., Landolt, D., 1997. Microstructure of Ni/Cu multilayers electrodeposited from a citrate electrolyte. Electrochimica Acta 42, 2407–2417. https://doi.org/10.1016/S0013-4686(97)82474-7.

Brunow, J., Gries, S., Krekeler, T., Rutner, M., 2022. Material mechanisms of Cu/Ni nanolaminate coatings resulting in lifetime extensions of welded joints. Scr. Mater. 212, 114501. https://doi.org/10.1016/j.scriptamat.2022.114501.

Brunow, J., Ritter, M., Krekeler, T., Rutner, M. Thermal Stability of a Nanolayered Metal Joint. *Scripta Materialia* 194 (2021) 113687. DOI: https://doi.org/10.1016/j.scriptamat.2020.113687.

Brunow, J., Rutner, M., 2021. Das Nanolaminatpflaster – Schweißnahtnachbehandlung für bisher unerreichte Lebensdauerverlängerung. Stahlbau 90, 691–700. https://doi.org/10.1002/stab.202100042.

Brunow, J., Spalek, N., Mohammadi, F., Rutner, M., 2023. A novel post-weld treatment using nanostructured metallic multilayer for superior fatigue strength. Sci. Rep. 13, 22215. https://doi.org/10.1038/s41598-023-49192-0.

Chason, E., Engwall, A., Pei, F., Lafouresse, M., Bertocci, U., Stafford, G., Murphy, J.A., Lenihan, C., Buckley, D.N., 2013. Understanding Residual Stress in Electrodeposited Cu Thin Films. J. Electrochem. Soc. 160, 3285–3289. https://doi.org/10.1149/2.048312jes.

Chason, E., Sheldon, B.W., Freund, L.B., Floro, J.A., Hearne, S.J., 2002. Origin of compressive residual stress in polycrystalline thin films. Phys. Rev. Lett. 88, 156103. https://doi.org/10.1103/PhysRevLett.88.156103.

Chmelko, V., Margetin, M., Harakal', M., 2018. Notch effect of welded joint. MATEC Web Conf. 165, 21003. https://doi.org/10.1051/matecconf/201816521003.
Clemens, B.M., Kung, H., Barnett, S.A., 1999. Structure and Strength of Multilayers. MRS Bull. 24, 20–26. https://doi.org/10.1557/S0883769400051502.
DIN 50100:2016-12: Schwingfestigkeitsversuch - Durchführung und Auswertung von zyklischen Versuchen mit konstanter Lastamplitude für metallische Werkstoffproben und Bauteile, 2016. . Beuth Verlag GmbH, Berlin. https://doi.org/10.31030/2580844.
DIN 50125:2022-08: Prüfung metallischer Werkstoffe - Zugproben, 2022. . Beuth Verlag GmbH, Berlin. https://doi.org/10.31030/3337825
DIN EN 1993-1-9:2010-12, Eurocode_3: Bemessung und Konstruktion von Stahlbauten_- Teil_1-9: Ermüdung; Deutsche Fassung EN_1993-1-9:2005_+ AC:2009, 2010. . DIN Media GmbH.
Engwall, A.M., Rao, Z., Chason, E., 2016. Origins of residual stress in thin films: Interaction between microstructure and growth kinetics. Mater. Des. 110, 616–623. https://doi.org/10.1016/j.matdes.2016.07.089.
Falah, M., Lau, R., Spalek, N., Lalkovski, N., Rutner, M., 2025. Significant improvement of the fatigue performance of ER70S-6 WAAM un-milled structures: A Cu/Ni multilayer nanotechnology approach. Struct. Integr. Procedia 67.
Haagensen, P.J., Maddox, S.J., 2013. IIW recommendations on methods for improving the fatigue strength of welded joints: IIW-2142-10, IIW document / International Institute of Welding. Woodhead Publ.; International Institute of Welding, Cambridge, UK; Philadelphia, PA.
Hensel, J., Eslami, H., Nitschke-Pagel, T., Dilger, K., 2019. Fatigue Strength Enhancement of Butt Welds by Means of Shot Peening and Clean Blasting. Metals 9, 744. https://doi.org/10.3390/met9070744.
Hensel, J., Nitschke-Pagel, T., Dilger, K., 2015. On the effects of austenite phase transformation on welding residual stresses in non-load carrying longitudinal welds. Weld. World 59, 179–190. https://doi.org/10.1007/s40194-014-0190-3.
Kim, I.-T., Jeong, Y.-S., 2013. Fatigue strength improvement of welded joints by blast cleaning for subsequent painting. Int. J. Steel Struct. 13, 11–20. https://doi.org/10.1007/s13296-013-1002-0.
Kuhlmann, U., Bergmann, J., Dürr, A., Thumser, R., Günther, H.-P., Gerth, U., 2005. Erhöhung der Ermüdungsfestigkeit von geschweißten höherfesten Baustählen durch Anwendung von Nachbehandlungsverfahren. Stahlbau 74, 358–365. https://doi.org/10.1002/stab.200590066.
Marquis, G.B., Barsoum, Z., 2016. IIW Recommendations on High Frequency Mechanical Impact (HFMI) Treatment for Improving the Fatigue Strength of Welded Joints, in: Marquis, Barsoum (Eds.), IIW Recommendations for the HFMI Treatment: For Improving the Fatigue Strength of Welded Joints, IIW Collection. Springer, Singapore, pp. 1–34. https://doi.org/10.1007/978-981-10-2504-4_1.
Nix, W.D., Clemens, B.M., 1999. Crystallite coalescence: A mechanism for intrinsic tensile stresses in thin films. J. Mater. Res. 14, 3467–3473. https://doi.org/10.1557/JMR.1999.0468.
Ramezani, M.G., Demkowicz, M.J., Feng, G., Rutner, M.P., 2017. Joining of physical vapor-deposited metal nano-layered composites. Scr. Mater. 139, 114–118. https://doi.org/10.1016/j.scriptamat.2017.06.032.
Rutner, M., Lalkovski, N., Falah, M., Seidelmann, M., Spalek, N., 2025. Merging nano and macro structure design: Opportunities for the structural integrity of steel infrastructure. Struct. Integr. Procedia 67.
Rutner, M., Spalek, N., Falah, M., Lalkovski, N., 2024. Verknüpfung von Nano mit Makro – Chancen für den Stahlbau. Stahlbau 93, 584–596. https://doi.org/10.1002/stab.202400048.
Scholtes, B., Vöhringer, O., 1993. Ursachen, Ermittlung und Bewertung von Randschichtveränderungen durch Kugelstrahlen. Mater. Werkst. 24, 421–431. https://doi.org/10.1002/mawe.19930241206.
Seidelmann, M., Spalek, N., Falah, M., Lalkovski, N., Rutner, M., 2025. Enhancing the Lifespan of Steel Structures through a 3D-printed Coating Container for the Application of a Nanometallic Multilayer on Weld Seams. Struct. Integr. Procedia 67.
Shugurov, A.R., Panin, A.V., 2020. Mechanisms of Stress Generation in Thin Films and Coatings. Tech. Phys. 65, 1881–1904. https://doi.org/10.1134/S1063784220120257.
Soyama, H., Chighizola, C.R., Hill, M.R., 2021. Effect of compressive residual stress introduced by cavitation peening and shot peening on the improvement of fatigue strength of stainless steel. J. Mater. Process. Technol. 288, 116877. https://doi.org/10.1016/j.jmatprotec.2020.116877.
Stoudt, M.R., Ricker, R.E., Cammarata, R.C., 2001. The influence of a multilayered metallic coating on fatigue crack nucleation. Int. J. Fatigue 23, 215–223. https://doi.org/10.1016/S0142-1123(01)00153-0.
Totten, G., 2008. Handbook of residual stress and deformation of steel, 3rd printing. ed. ASM International, Materials Park, Ohio.
Trojan, K., Hervoches, C., Kolařík, K., Ganev, N., Mikula, P., Čapek, J., 2017. REAL STRUCTURE AND RESIDUAL STRESSES IN ADVANCED WELDS DETERMINED BY X-RAY AND NEUTRON DIFFRACTION. Acta Polytech. CTU Proc. 9, 32. https://doi.org/10.14311/APP.2017.9.0032.
Ummenhofer, T., Herion, S., Weich, I., 2009. Schweißnahtnachbehandlung mit höherfrequenten Hämmerverfahren – Ermüdungsfestigkeit, Qualitätssicherung, Bemessung. Stahlbau 78, 605–612. https://doi.org/10.1002/stab.200910074.
Ummenhofer, T., Weich, I., Nitschke-Pagel, T., 2005. Lebens- und Restlebensdauerverlängerung geschweißter Windenergieanlagentürme und anderer Stahlkonstruktionen durch Schweißnahtnachbehandlung. Stahlbau 74, 412–422. https://doi.org/10.1002/stab.200590085.
Wang, Y.-C., Misra, A., Hoagland, R.G., 2006. Fatigue properties of nanoscale Cu/Nb multilayers. Scr. Mater. 54, 1593–1598. https://doi.org/10.1016/j.scriptamat.2006.01.027.
Woelke, P.B., Rutner, M.P., Shields, M.D., Rans, C., Alderliesten, R., 2015. Finite Element Modeling of Fatigue in Fiber–Metal Laminates. AIAA J. 53, 2228–2236. https://doi.org/10.2514/1.J053600.
Zhu, X.F., Zhang, G.P., 2009. Tensile and fatigue properties of ultrafine Cu–Ni multilayers. J. Phys. Appl. Phys. 42, 055411. https://doi.org/10.1088/0022-3727/42/5/055411.